Fabrication of high-quality ZnS buffer and its application in Cd-free CIGS solar cells*

LI Feng-yan (李凤岩)[1], **DANG Xiang-yu** (党向瑜)[1], **ZHANG Li** (张力)[1]**, **LIU Fang-fang** (刘芳芳)[1], **SUN Ding** (孙顶)[1], **HE Qing** (何青)[1], **LI Chang-jian** (李长健)[1], **LI Bao-zhang** (李宝璋)[1], **and ZHU Hong-bing** (朱红兵)[2]

1. Tianjin Key Laboratory for Photoelectronic Thin Film Devices and Technology, Nankai University, Tianjin 300071, China

2. College of Physics Science & Technology, Hebei University, Baoding 071002, China

(Received 18 April 2014)

This paper provides the fabrication of Cd-free Cu(In,Ga)Se_2 (CIGS) solar cells on soda-lime glass substrates. A high quality ZnS buffer layer is grown by chemical bath deposition (CBD) process with $ZnSO_4$-NH_3-SC $(NH_2)_2$ aqueous solution system. The X-ray diffraction (XRD) result shows that the as-deposited ZnS film has cubic (111) and (220) diffraction peaks. Scanning electron microscope (SEM) images indicate that the ZnS film has a dense and compact surface with good crystalline quality. Transmission measurement shows that the optical transmittance is about 90% when the wavelength is beyond 500 nm. The bandgap (E_g) value of the as-deposited ZnS film is estimated to be 3.54 eV. Finally, a competitive efficiency of 11.06% is demonstrated for the Cd-free CIGS solar cells with ZnS buffer layer after light soaking.

Document code: A **Article ID:** 1673-1905(2014)04-0266-3

DOI 10.1007/s11801-014-4064-0

Chalcopyrite-based Cu(In,Ga)Se_2 (CIGS) thin film solar cells have been considered as one of the most promising solar cells for cost-effective power generation. Currently, the best efficiency of 20.4% has been demonstrated, which is comparable with that of the best multi-crystalline silicon cells[1-3]. These high efficiency devices are typically fabricated by using a high-toxic cadmium sulfide buffer layer deposited by chemical bath deposition (CBD) process. It is reported that CdS buffer layer can protect the pn junction region from sputtering damage during the sequent ZnO deposition[4-6]. In spite of this, previous work by Jiang et al, which is on the built-in electrical potential of CIGS solar cells by using the scanning Kelvin probe microscopy, suggests that the pn junction is a buried homojuction located in the CIGS film and 30–80 nm from the CdS/CIGS interface[7,8]. This is a result that the CIGS surface layer is inverted n-type from p-type by Cd^{2+} doping. However, environmental concerns and hazards related to the heavy metal Cd element should be considered during mass production of CIGS modules. Additionally, the quantum efficiency of CdS/CIGS solar cells is decreased at short wavelengths due to the optical absorption from the CdS layer. Therefore, it is necessary to replace CdS (E_g=2.4 eV) with wider bandgap alternative buffer layers. ZnS film with bandgap energy of about 3.8 eV has been considered as an ideal alternative buffer layer for high efficiency Cd-free CIGS solar cells[9,10].

In our previous study, the CIGS thin film solar cells with the conversion efficiency over 15% have been reported[11]. Based on the high quality CIGS absorber layer, we try to fabricate Cd-free CIGS thin film solar cells in this paper.

CIGS thin films were deposited onto the Mo coated soda-lime glass (SLG) substrate by co-evaporation process from the independently controlled Cu, In, Ga and Se sources[12]. In the first stage, an In-Ga-Se precursor was deposited onto the substrate at about 350 °C. Subsequently, the precursor was exposed to Cu and Se fluxes to form Cu-rich CIGS films. In the third stage, small amounts of In, Ga and Se were evaporated to form slightly Cu-poor CIGS film. During the second and the third stages, the substrate temperatures were kept at 450 °C. Typical thickness of the CIGS films is from 1.5 μm to 2.5 μm. The chemical composition of the films was determined by X-ray fluorescent spectrometer (XRF-800) with an Rh-anode. The optical transmittance and reflectance were measured by a Cary 5000 UV-VIS-NIR spectrophotometer. Spectral resolution for optical transmission was measured at UV-VIS range ($\lambda \leq$ 0.048 nm) and

* This work has been supported by the Fundamental Research Funds for the Central Universities (No.65011991), and the Specialized Research Fund for the Doctoral Program of Higher Education (No.BE033511).

** E-mail: lzhang@nankai.edu.cn

NIR range ($\lambda \leq$ 0.2 nm). The surface morphologies were measured by JEOL JSM-6700 scanning electron microscopy (SEM). The solar cell of Al/ZnO/CdS or ZnS/CIGS was completed by the standard process[13,14]. The current density-voltage (*J-V*) measurements were performed under the standard AM1.5 spectrum for 100 mW/cm^2 at 25 °C after a light soaking for 20 min. The light source of solar simulator was calibrated by a standard single crystal Si solar cell.

ZnS buffer layers were grown on CIGS absorber using $ZnSO_4$-NH_3-$SC(NH_2)_2$ aqueous solutions at different temperatures from 60 °C to 80 °C by a chemical bath deposition (CBD) process. 15 mL N_2H_4 (80%) solution was used as complexant. By optimizing the deposition conditions (deposition temperature, growth duration and solution concentration), ZnS layer with thickness of about 70 nm was prepared. And the optimum deposition parameters are summarized in Tab.1.

Tab.1 Optimum deposition parameters of ZnS buffer layer via CBD process

Solution	Concentration (mol/L)	Deposition temperature (°C)	Growth duration (min)
$ZnSO_4$	0.025–0.300		
$SC(NH_2)_2$	0.25–0.30	81	20–30
Ammonia	2.5–3.0		

At the beginning of the reaction, $NH_3 \cdot H_2O$ and $N_2H_4 \cdot H_2O$ possibly combine with Zn^{2+} to form complex ions, which greatly reduces the concentration of free Zn^{2+} in the solution:

$$Zn^{2+}+4NH_3 \leftrightarrow [Zn(NH_3)_4]^{2+}, \quad (1)$$

$$Zn^{2+}+3N_2H_4 \leftrightarrow [Zn(N_2H_4)_3]^{2+}. \quad (2)$$

$NH_3 \cdot H_2O$ and $N_2H_4 \cdot H_2O$ hydrolyze in the aqueous solution to form an alkaline environment as

$$NH_3 \cdot H_2O \leftrightarrow NH_4^+ + OH^-, \quad (3)$$

$$N_2H_4 \cdot H_2O \leftrightarrow N_2H_5^+ + OH^-. \quad (4)$$

Thiourea is used as the S^{2-} source through hydrolysis in alkaline medium:

$$SC(NH_2)_2 + 3OH^- \rightarrow CO_3^{2-} + HS^- + 2NH_3, \quad (5)$$

$$HS^- + OH^- \rightarrow S^{2-} + 2H_2O. \quad (6)$$

$[Zn(N_2H_4)_3]^{2+}$ complex ions with stability constant k=$10^{5.5}$ are more stable than $[Zn(NH_3)_4]^{2+}$ with k=$10^{8.9}$. Thus, $[Zn(NH_3)_4]^{2+}$ is the major precursor in the heterogeneous growth of ZnS thin films. The overall reaction of ZnS thin films can be given as

$$[Zn(NH_3)_4]^{2+}+SC(NH_2)_2+2OH^- \leftrightarrow$$

$$ZnS_{substrate}+3NH_3+CH_2N_2+2H_2O. \quad (7)$$

When Zn^{2+} and S^{2-} concentration product is greater than the solubility product of ZnS, the precipitation in solution instead of heterogeneous reaction takes place.

X-ray diffraction (XRD) of ZnS grown on SLG substrate was measured with the θ–2θ mode using CuKα radiation, as shown in Fig.1. The XRD pattern shows mainly cubic (111) and (220) ZnS diffraction peaks. Compared with the results from Ref.[15], our ZnS film has good crystalline quality with sharp (111) peak.

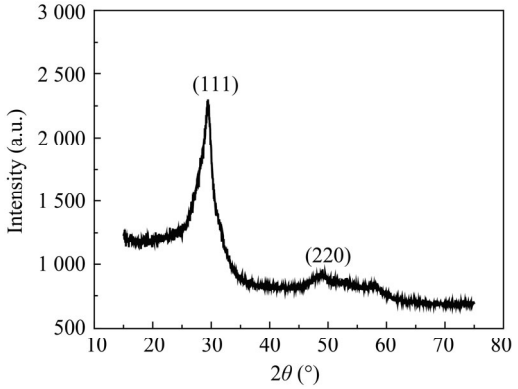

Fig.1 XRD pattern of the as-deposited ZnS films

Fig.2 shows the SEM morphology of ZnS film grown by our process. The ZnS film shows a compact and uniform structure with better crystalline quality, which is consistent with the XRD result.

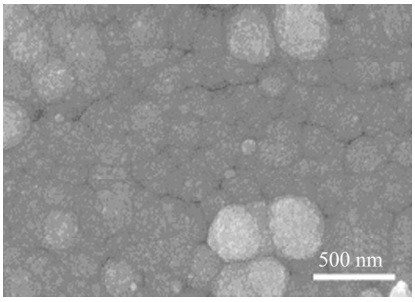

Fig.2 Surface morphology of the as-deposited ZnS films

The optical transmission spectrum of ZnS film grown on SLG substrate with thickness of about 70 nm is shown in Fig.3. We can see from Fig.3 that the transmission of the as-deposited film is greater than 90% in the visible range. The high optical transmittance can be utilized with buffer layer for CIGS thin film solar cells.

The absorption coefficient α is analyzed for near-edge optical absorption of semiconductors by using

$$\alpha h\nu = k(h\nu - E_g)^{n/2}, \quad (8)$$

where k is constant and n is a constant that is equal to 1 for direct bandgap semiconductors. The bandgap E_g is determined from the intercept of the straight-line portion of $(\alpha h\nu)^2$. The inset of Fig.3 shows the relation between $(\alpha h\nu)^2$ and the incident radiation energy $h\nu$. E_g about 3.54 eV can be calculated from the linear fitting, which is consistent with other results [15,16].

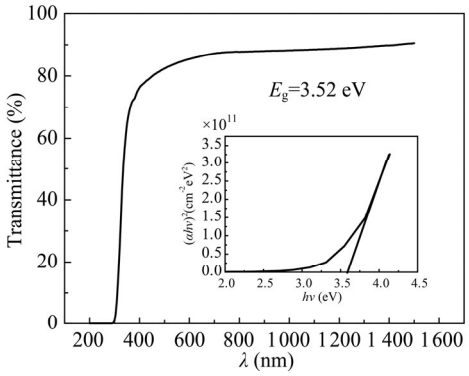

Fig.3 Transmission spectrum of the as-deposited ZnS films

We made CIGS solar cells with an active area of 1 cm^2 by using CdS and ZnS as buffer layer, respectively. CIGS films with compositional ratios Cu/III of 0.94 and Ga/III of 0.32 were applied to the device preparation. The conversion efficiency of 11.06% is obtained for the CIGS solar cell with ZnS buffer after light soaking, and the parameters are short current density J_{sc}=32.9 mA/cm^2, open circuit voltage V_{oc}=480.0 mV and fill factor FF=71%. Such an efficient Cd-free CIGS solar cell should be related to the better structural and optical properties of our ZnS buffer. The CIGS solar cell with CdS buffer has the following cell parameters: J_{sc}=28.2 mA/cm^2, V_{oc}=594.8 mV, FF=73.1% and η=12.3%. Compared with CdS buffer, the device parameters of CIGS cells with ZnS buffer are limited by their relatively low V_{oc} and FF. V_{oc} may be dominated by the more recombination occurring in CIGS/ZnS interface because of no buried pn junction and big conduction band offset between CIGS and ZnS[17]. Further investigation is required to understand the discrepancy.

Fig.4 shows the comparison of the external quantum efficiency (EQE) data of the CIGS devices with CdS and ZnS buffer layers. As can be seen clearly in Fig.4, the quantum efficiency of the device utilizing a CBD-ZnS buffer layer is higher than that of the device using a CBD-CdS buffer in 400–500 nm range since CBD-ZnS has a wider bandgap than CBD-CdS (2.4 eV), which results in an increased value of J_{sc}. The small difference in cut-off wavelength at approximately 1 100 nm is attributed to the difference in junction characterization[11].

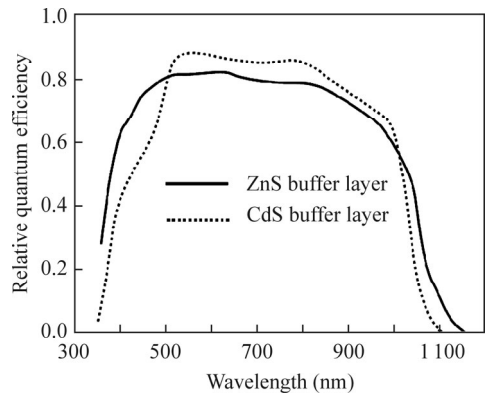

Fig.4 EQEs of the CIGS solar cells with CdS buffer and ZnS buffer

In conclusion, a high quality ZnS buffer layer is successfully fabricated by CBD process. Structural and optical properties are characterized by XRD, SEM and transmittance spectra measurements. The as-deposited ZnS film indicates cubic (111) and (220) ZnS diffraction peaks and a dense and compact surface with good crystalline quality from XRD and SEM results. The optical transmittance is about 90% for the wavelength range above 500 nm, indicating a highly transparent film. The bandgap (E_g) for ZnS buffer layer is about 3.54 eV. A competitive efficiency of 11.06% is obtained for Cd-free CIGS solar cells with ZnS buffer layer after light soaking.

Acknowledgements

The authors express their sincere appreciation to Dr. Liu Qi for her help with kind discussion.

References

[1] Green M. A., Emery K., Hishikawa Y., Warta W. and Dunlop E. D., Progress in Photovoltaics: Research and Applications **21**, 827 (2013).

[2] LI Bo-yan, ZHANG Yi, LIU Wei and SUN Yun, Optoelectronics Letters **8**, 348 (2012).

[3] XIN Zhi-yun, CHEN Xi-ming, QIAO Zai-xiang, WANG He, XUE Yu-ming, PAN Zhen and TIAN Yuan, Optoelectronics Letters **9**, 112 (2013).

[4] Orgassa K., Rau U., Nguyen Q., Schock H. W. and Werner J. H., Progress in Photovoltaics: Research and Applications **10**, 451 (2002).

[5] Nakada T. and Kunioka A., Applied Physics Letters **74**, 444 (1999).

[6] Nakada T., Thin Solid Films **361-362**, 346 (2000).

[7] Jiang C. S., Hasoon F. S., Moutinho H. R., Al-Thani H. A., Romero M. J. and Al-Jassim M. M., Applied Physics Letters **82**, 127 (2003).

[8] Yan Y., Jones K. M., Abushama J., Young M., Asher S., Al-Jassim M. M. and Noufi R., Applied Physics Letters **81**, 1008 (2002).

[9] Nakada T. and Mizutani M., Japanese Journal of Applied Physics **41**, L165 (2002).

[10] Bhattacharya R. N., Contreras M. A. and Teeter G., Japanese Journal of Applied Physics **43**, L1475 (2004).

[11] Liu F. F., Zhang L. and He Q., Acta Phys. Sin. **62**, 077201 (2012). (in Chinese)

[12] Zhang L., He. Q, Jiang W. L., Li C. J. and Sun Y., Chinese Physics Letter **26**, 026801 (2009).

[13] Zhang L., He Q., Jiang W. L., Liu F. F., Li C. J. and Sun Y., Solar Energy Materials and Solar Cells **43**, 93 (2009).

[14] Zhang L., Liu F. F., Li F. Y., He Q., Li B. Z. and Li C. J., Solar Energy Materials and Solar Cells **99**, 356 (2012).

[15] Liu Q., Mao G. B. and Ao J. P., Applied Surface Science **254**, 5711 (2008).

[16] Oladeji I. O. and Chow L., Thin Solid Films **339**, 148 (1999).

[17] Nakada T., Hongo M. and Hayashi E., Thin Solid Films **431-432**, 242 (2003).